Journal of Sound and Vibration 329 (2010) 4124–4135

Contents lists available at ScienceDirect

Journal of Sound and Vibration

journal homepage: www.elsevier.com/locate/jsvi

Active control of power flow transmission in finite connected plate

Chun-Chuan Liu [a], Feng-Ming Li [a,*], Bo Fang [a], Yang Zhao [b], Wen-Hu Huang [a]

[a] School of Astronautics, Harbin Institute of Technology, P.O. Box 137, Harbin 150001, PR China
[b] School of Astronautics, Harbin Institute of Technology, P.O. Box 359, Harbin 150001, PR China

ARTICLE INFO

Article history:
Received 1 December 2009
Received in revised form
10 March 2010
Accepted 25 April 2010
Handling Editor: L.G. Tham
Available online 23 May 2010

ABSTRACT

The vibration propagation and active control of power flow in finite connected plate structure are studied. The dynamic response of the connected plate is obtained by the wave approach. The active power flow at the junction of the connected plate is suppressed by the feedforward active vibration control. It indicates that the active power flow at the junction of the connected plate cannot be well suppressed by the optimal control force for minimizing the acceleration, but it can be effectively suppressed by the optimal control force for minimizing the active power flow. The small error of the optimal control force has slight effects on the control results.

1. Introduction

The connected rectangular plate structures are usually used in many engineering applications such as the satellite structures and ship hulls. Disturbance produced in these structures by the external excitation can propagate through the junction of the connected plate structures. For example, the high speed reaction flywheel in satellite can produce median and high frequency disturbances that can transmit through the junction of the satellite structure and the disturbances can influence the positioning accuracy and imaging quality of the photographic camera in the satellite. Therefore, it is necessary to study the disturbance propagation and vibration suppression of the connected rectangular plate structure.

The power flow model can be used to describe the vibration propagation in structures [1–14]. The active power represents the time-average power in a vibration cycle and it corresponds to the local net transport of disturbance energy. Noiseux [1] used the active power to describe the energy transporting from one part of the structure to another. Romanoa et al. [3] presented a generalized formulation of the structure power flow, or the Poynting vector for thin elastic shells and plates. He gave the Poynting vector formulation in different coordinates, and obtained the relationship between the energy and power flow in different coordinates. He proved that the vibratory strength of shells and plates could be estimated by structure power flow.

Mace [4,5] calculated the distribution of structural power flow with statistic energy analysis (SEA) approach. He studied the power transmission in one-dimensional beamlike coupled structures and two-dimensional plate-like structures and estimated the structural coupled loss factors by combining wave approach with SEA method. Cuschieri et al. [6–10] presented the mobility power flow approach (MPA). The input and transmitted powers can be calculated by the structure mobility functions to analyze the response of L-shaped plate in mid-frequencies. And the active power flow was used to represent the transmission of vibratory energy in the finite L-shaped plate. The input power from the disturbance sources and the transmitted power through coupled joints can be obtained.

Kessissoglou [11] calculated the active power flow of an L-shaped plate in the median and high frequency regions and the in-plane longitudinal and shear waves were considered in the power flow calculation. She found that these in-plane

* Corresponding author. Tel.: +86 451 86414479.
E-mail addresses: fmli@hit.edu.cn, lfmcy@yahoo.com (F.-M. Li).

0022-460X/$ - see front matter © 2010 Elsevier Ltd. All rights reserved.
doi:10.1016/j.jsv.2010.04.027

motions had significant effects on the power flow in median and high frequencies. Choi et al. [12] gave a higher-order sandwich theory in conjunction with an equivalent mobility-based power flow progressive approach to determine power flow for a sandwich configured floating raft vibration isolation system. He found that the loss factors of the sandwich configured floating raft could influence effectively the power flow transmitted to the foundation in the median and high frequencies. Yan et al. [13,14] studied the power flow transmitting in a submerged infinite cylindrical shell reinforced by supports of rings and bulkheads. The input vibrational active power flow into the structure was calculated and the influences of different structural parameters on the results were discussed.

The active vibration control has been used extensively to suppress the active power flow in beams [15–19]. Pan and Hansen [15] analyzed the physical control model of the total power for the bending, torsional and longitudinal waves in the infinite beams. They considered that only the active power could travel to the far field in the infinite beams, while the reactive component power could only exist in the local oscillation, and could not propagate to the far field of infinite beams. Pan and Hansen [16] researched the effect of the locations and type of error sensor on the active control of vibrational power flow in infinite beam. They used the vibration amplitude as the cost function for the active control of the vibrational power transmission in the infinite beam. Schwenk et al. [17] studied an algorithm to control adaptively the structural vibration intensity in a beam. A number of control actuators and error sensors were use to investigate the effectiveness of adaptive control of structural intensity. And the effect by controlling the intensity was compared to that by controlling the acceleration.

Audrain et al. [18] investigated the active structural intensity control in finite beams based on theory and experiment. The instantaneous intensity was completely taken into account in the control algorithm. These results approved that active intensity control could preserve a good control performance when error sensors were placed in the near field of the control source and the primary disturbance. Pereira et al. [19] used an active control method based on minimizing the active part of the structural intensity to reduce the overall vibration level in beams. They considered that the control forces dissipated the input power due to the perturbing forces. Pan and Hansen [20] researched the active control of harmonic vibratory power transmission along a semi-infinite plate. They calculated and compared the effects of the optimal control force for minimizing the active power flow and acceleration in a certain position of the plate. It was shown that the location of control force influenced very much to the active control of vibrational power flow transmission in the plate.

Although much attention has been paid to the power flow of the beam- and plate-like structures, to our knowledge, there has been no published work on the active control of power flow transmission through the junction of the finite closed connected plate structure in the open literatures. Previous works on the active control of power flow transmission in structures mainly focus on the beams [15–19] and semi-infinite plates [20].

In this paper, the wave propagation and active vibration control in finite closed connected plates are investigated using wave approach. The dynamic responses at specific locations of connected plate structure for median and high frequency excitations are obtained by the wave method. The active control based on the structural active power flow is used to suppress the energy propagation at the junction of the coupled plate structure. In the numerical calculation, the active power at the junction of closed connected plate structure and L-shaped plate are suppressed by active control, respectively, and the influence of the error of the control force on the control results is considered. It is seen that the active power flow transmitted through the junction of the connected plate can be effectively suppressed by the active control.

2. Dynamic response

A closed connected plate structure as shown in Fig. 1 is considered. The structure consists of four plates, and each plate is simply supported along two parallel edges corresponding to $y=0$ and L_y. The length of the coupled plates are L_1, L_2, L_3 and L_4, respectively. The material and thickness of the four plates are the same. The dynamics model of the plate can be expressed as

$$D\nabla^4 w+\rho h\frac{\partial^2 w}{\partial t^2}=f(x,y,t), \tag{1}$$

where ρ is the material density, h is the thickness, $D=Eh^3/[12(1-v^2)]$ is the flexural rigidity, E and v are Young's modulus and Poisson's ratio of the plate, and $f(x,y,t)$ is the external excitation.

For the simply supported boundary edges, the transverse displacement of the plate can be given by

$$w(x,y,t)=\sum_{n=1}^{\infty}[A_1\,e^{ik_x x}+A_2\,e^{k_{nx}x}+A_3\,e^{-ik_x x}+A_4\,e^{-k_{nx}x}]\sin k_y y\,e^{i\omega t}, \tag{2}$$

where w is out-of-plane displacement of the plate, A_1, A_2, A_3 and A_4 are the wave displacement amplitudes, $k_y=n\pi/L_y$ is the modal wavenumber in the y direction, $k_x=\sqrt{k_F^2-k_y^2}$ and $k_{nx}=\sqrt{k_F^2+k_y^2}$ are the wavenumbers in the x direction for the travelling and evanescent waves, where $k_F=\sqrt[4]{\rho h/D}\sqrt{\omega}$ is the plate flexural wavenumber and ω is the circular frequency. The harmonic dynamic factor $e^{i\omega t}$ is generally contained in the expressions for the wave approach. So the harmonic dynamic factor $e^{i\omega t}$ in Eq. (2) is omitted in the followings.

Generally speaking, the in-plane displacement is very small compared to the out-of-plane one. There exists the wave mode transition between the flexural and in-plane waves at the joint of the closed coupled plate structure. The in-plane

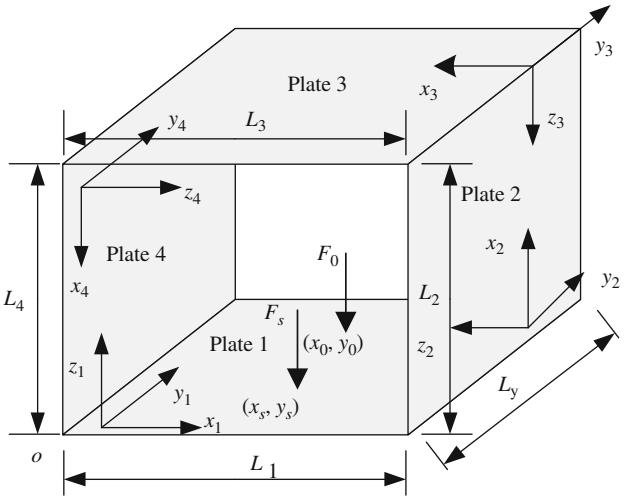

Fig. 1. The schematic diagram of □-shaped connected plate structure

wave motion should be considered in the calculation of the power flow for the closed plate structure [11]. The equations of in-plane motion are [10,21]

$$\frac{\partial^2 u}{\partial x^2}+\frac{1-\nu}{2}\frac{\partial^2 u}{\partial y^2}+\frac{1+\nu}{2}\frac{\partial^2 v}{\partial x\partial y}+\frac{(1-\nu^2)\rho}{E}\omega^2 u=0, \tag{3}$$

$$\frac{\partial^2 v}{\partial y^2}+\frac{1-\nu}{2}\frac{\partial^2 v}{\partial x^2}+\frac{1+\nu}{2}\frac{\partial^2 u}{\partial x\partial y}+\frac{(1-\nu^2)\rho}{E}\omega^2 v=0, \tag{4}$$

where $u(x,y)$ is the in-plane longitudinal displacement, and $v(x,y)$ is the in-plane shear displacement. For the simply supported plates along the longitudinal edges, the in-plane longitudinal and in-plane shear displacements can be expressed as [11,21]

$$u(x,y)=\sum_{n=1}^{\infty}(\lambda_1 B_1 e^{\lambda_1 x}+\lambda_2 B_2 e^{\lambda_2 x}+k_y B_3 e^{\lambda_3 x}+k_y B_4 e^{\lambda_4 x})\sin k_y y, \tag{5}$$

$$v(x,y)=\sum_{n=1}^{\infty}(k_y B_1 e^{\lambda_1 x}+k_y B_2 e^{\lambda_2 x}+\lambda_3 B_3 e^{\lambda_3 x}+\lambda_4 B_4 e^{\lambda_4 x})\cos k_y y, \tag{6}$$

where $\lambda_{1,2}=\pm\sqrt{k_y^2-k_L^2}$ and $\lambda_{3,4}=\pm\sqrt{k_y^2-k_S^2}$ are the eigenvalues of the in-plane displacement solutions, and $k_L=\omega\sqrt{\rho(1-\nu^2)/E}$ and $k_S=\omega\sqrt{2\rho(1+\nu)/E}$ are the longitudinal and shear wavenumbers. The dynamic response of plate can be exactly determined by Eqs. (2), (5) and (6), but there exists the cut-on frequencies in the wave solutions of the plate [20]. In order to calculate accurately the dynamic response in median and high frequencies, the minimized mode number should be taken as $N_B=(L_xL_y/2h)\sqrt{12\rho(1-\nu^2)/E}(2\pi\omega)$ (number of banding modes), $N_L=[\pi L_xL_y\rho(1-\nu^2)/E](2\pi\omega)^2$ (number of in-plane longitudinal modes), $N_S=[\pi L_xL_y2\rho(1+\nu)/E](2\pi\omega)^2$ (number of in-plane shear modes) [11].

The dynamic response of the closed coupled plate structure as shown in Fig. 1 can be analyzed by combining the wave method and substructure approach. Considering the disturbance force as the continuous conditions, the flexural and in-plane displacements in plate 1 can be expressed as

$$w_{1I}(x_1,y_1)=\sum_{n=1}^{\infty}[A_1e^{ik_{nx}x_1}+A_2e^{k_{nx}x_1}+A_3e^{-ik_{nx}x_1}+A_4e^{-k_{nx}x_1}]\sin k_y y_1,\quad 0\le x_1<x_0, \tag{7}$$

$$w_{1II}(x_1,y_1)=\sum_{n=1}^{\infty}[A_5e^{ik_{nx}x_1}+A_6e^{k_{nx}x_1}+A_7e^{-ik_{nx}x_1}+A_8e^{-k_{nx}x_1}]\sin k_y y_1,\quad x_0\le x_1<L_1, \tag{8}$$

$$u_1(x_1,y_1)=\sum_{n=1}^{\infty}(\lambda_1 B_1 e^{\lambda_1 x_1}+\lambda_2 B_2 e^{\lambda_2 x_1}+k_y B_3 e^{\lambda_3 x_1}+k_y B_4 e^{\lambda_4 x_1})\sin k_y y_1, \tag{9}$$

$$v_1(x_1,y_1)=\sum_{n=1}^{\infty}(k_y B_1 e^{\lambda_1 x_1}+k_y B_2 e^{\lambda_2 x_1}+\lambda_3 B_3 e^{\lambda_3 x_1}+\lambda_4 B_4 e^{\lambda_4 x_1})\cos k_y y_1. \tag{10}$$

The flexural and in-plane displacements in plate 2 can be expressed as

$$w_2(x_2,y_2)=\sum_{n=1}^{\infty}[A_9e^{ik_xx_2}+A_{10}e^{k_{nx}x_2}+A_{11}e^{-ik_xx_2}+A_{12}e^{-k_{nx}x_2}]\sin k_yy_2,\quad 0\le x_2<L_2, \tag{11}$$

$$u_2(x_2,y_2)=\sum_{n=1}^{\infty}(\lambda_1B_5e^{\lambda_1x_2}+\lambda_2B_6e^{\lambda_2x_2}+k_yB_7e^{\lambda_3x_2}+k_yB_8e^{\lambda_4x_2})\sin k_yy_2, \tag{12}$$

$$v_2(x_2,y_2)=\sum_{n=1}^{\infty}(k_yB_5e^{\lambda_1x_2}+k_yB_6e^{\lambda_2x_2}+\lambda_3B_7e^{\lambda_3x_2}+\lambda_4B_8e^{\lambda_4x_2})\cos k_yy_2, \tag{13}$$

The flexural and in-plane displacement in plate 3 can be expressed as

$$w_3(x_3,y_3)=\sum_{n=1}^{\infty}[A_{13}e^{ik_xx_3}+A_{14}e^{k_{nx}x_3}+A_{15}e^{-ik_xx_3}+A_{16}e^{-k_{nx}x_3}]\sin k_yy_3,\quad 0\le x_3<L_3, \tag{14}$$

$$u_3(x_3,y_3)=\sum_{n=1}^{\infty}(\lambda_1B_9e^{\lambda_1x_3}+\lambda_2B_{10}e^{\lambda_2x_3}+k_yB_{11}e^{\lambda_3x_3}+k_yB_{12}e^{\lambda_4x_3})\sin k_yy_3, \tag{15}$$

$$v_3(x_3,y_3)=\sum_{n=1}^{\infty}(k_yB_9e^{\lambda_1x_3}+k_yB_{10}e^{\lambda_2x_3}+\lambda_3B_{11}e^{\lambda_3x_3}+\lambda_4B_{12}e^{\lambda_4x_3})\cos k_yy_3 \tag{16}$$

and the flexural and in-plane displacements in plate 4 can be expressed as

$$w_4(x_4,y_4)=\sum_{n=1}^{\infty}[A_{17}e^{ik_xx_4}+A_{18}e^{k_{nx}x_4}+A_{19}e^{-ik_xx_4}+A_{20}e^{-k_{nx}x_4}]\sin k_yy_4,\quad 0\le x_4<L_4, \tag{17}$$

$$u_4(x_4,y_4)=\sum_{n=1}^{\infty}(\lambda_1B_{13}e^{\lambda_1x_4}+\lambda_2B_{14}e^{\lambda_2x_4}+k_yB_{15}e^{\lambda_3x_4}+k_yB_{16}e^{\lambda_4x_4})\sin k_yy_4, \tag{18}$$

$$v_4(x_4,y_4)=\sum_{n=1}^{\infty}(k_yB_{13}e^{\lambda_1x_4}+k_yB_{14}e^{\lambda_2x_4}+\lambda_3B_{15}e^{\lambda_3x_4}+\lambda_4B_{16}e^{\lambda_4x_4})\cos k_yy_4, \tag{19}$$

where A_j (j=1, …, 20) and B_j (j=1, …, 16) are the flexural and in-plane displacement amplitude coefficients, which can be determined by 36 equations from the continuous and coupling conditions. There are four continuous equations at the applying force position [20] and 32 continuous equations at the coupling junctions of the plates. For the symmetry of the closed connected plate structure, there are eight coupling equations at the junction of every two consecutive plates. For the junction of the plates 2 and 3, the continuous conditions can be written as [11]

$$M_{xx2}=M_{xx3},\quad \frac{\partial w_{xx2}}{\partial x_2}=\frac{\partial w_{xx3}}{\partial x_3}, \tag{20,21}$$

$$w_2=u_3,\quad w_3=-u_2, \tag{22,23}$$

$$Q_{x2}+\frac{\partial M_{xy2}}{\partial x_2}=N_{xx3},\quad Q_{x3}+\frac{\partial M_{xy3}}{\partial x_2}=-N_{xx2}, \tag{24,25}$$

$$v_2=v_3,\quad N_{xy2}=N_{xy3}, \tag{26,27}$$

where M_{xx} is the bending moment, Q_x is the out-of-plane shear force, M_{xy} is the twist moment, N_{xx} is the in-plane longitudinal force, and N_{xy} is the in-plane shear force. The expressions of M_{xx}, Q_x, M_{xy}, N_{xx} and N_{xy} are written as

$$M_{xx}=-D\left(\frac{\partial^2w}{\partial x^2}+v\frac{\partial^2w}{\partial y^2}\right), \tag{28}$$

$$Q_x=-D\left(\frac{\partial^3w}{\partial x^3}+\frac{\partial^3w}{\partial x\partial y^2}\right), \tag{29}$$

$$M_{xy}=-D(1-v)\frac{\partial^2w}{\partial x\partial y}, \tag{30}$$

$$N_{xx}=\frac{Eh}{(1-v^2)}\left(\frac{\partial u}{\partial x}+v\frac{\partial v}{\partial y}\right), \tag{31}$$

$$N_{xy}=\frac{Eh}{2(1+v)}\left(\frac{\partial u}{\partial y}+\frac{\partial v}{\partial x}\right). \tag{32}$$

The continuous equations at other coupling junctions are similar to Eqs. (20)–(27).

Considering the coupling conditions at the junctions of different plates and the continuous conditions at the position where the force is applied, the matrix equation concerning to the displacement amplitude coefficients can be written as

$$[\alpha]\{A\}=\{F\}, \tag{33}$$

where $[\alpha]$ is a 36×36 matrix which consists of the coupling and continuous conditions, A and F are the displacement amplitude coefficients and force matrices, respectively, and are given by

$$\{A\}=\{A_1,A_2,A_3,A_4,A_5,A_6,A_7,A_8,A_9,A_{10},A_{11},A_{12},A_{13},A_{14},A_{15},A_{16},A_{17},A_{18},A_{19},A_{20},\\ B_1,B_2,B_3,B_4,B_5,B_6,B_7,B_8,B_9,B_{10},B_{11},B_{12},B_{13},B_{14},B_{15},B_{16}\}^T, \tag{34}$$

$$\{F\}=\left\{0,0,0,0,0,0,0,0,\frac{-2F_0}{L_yD}\sin k_y y_0,0,0,0,0,0,0,0,0,0,0,0,0,0,0,0,0,0,0,0,0,0,0,0,0,0,0,0,0,0,0,0\right\}^T. \tag{35}$$

The displacement amplitude coefficient matrix A can be determined from Eq. (33). The displacement responses at arbitrary position of the closed plate structure generated by the disturbance source $\vec{F}_0$ acting at the position (x_0,y_0) is given by

$$w_0(x,y)=w_{x0}(x,y)F_0,\quad u_0(x,y)=u_{x0}(x,y)F_0,\quad v_0(x,y)=v_{x0}(x,y)F_0, \tag{36a,b,c}$$

where $w_{x0}(x,y)$, $u_{x0}(x,y)$ and $v_{x0}(x,y)$ are the flexural and in-plane displacement responses generated by the unit force acting at position x_0. While the displacement responses generated by the active control force $\vec{F}_s$ acting at the position (x_s,y_s) is given by

$$w_s(x,y)=w_{xs}(x,y)F_s,\quad u_s(x,y)=u_{xs}(x,y)F_s,\quad v_s(x,y)=v_{xs}(x,y)F_s, \tag{37a,b,c}$$

where the meaning and form of $w_{xs}(x,y)$, $u_{xs}(x,y)$ and $v_{xs}(x,y)$ are the same as those of $w_{x0}(x,y)$, $u_{x0}(x,y)$ and $v_{x0}(x,y)$, but only the continuous conditions of the location at which the force $\vec{F}_s$ is applied are different.

3. Active control of the power flow

The feedforward active control approach which has been used to control the power transmitted in the beams [18] and semi-plates [20] is employed in this paper. A single control force is considered since only slight improvement of the control result can be obtained at some frequencies by increasing the number of the control actuators [22]. The controller which uses a filtered-x, feedforward, least-mean-square (LMS) and adaptive algorithm can implement the suppression of vibratory power transmission through the structure [23]. The active power flow at the junction of the plates is used as the cost function, which represents the time-average energy transmitted through the junction between the plates [6–10]. The active power flow through the section at the constant x is then given by [20]

$$\bar{I}_{x\alpha}=-\frac{1}{2}\int_0^{L_y}\mathrm{Re}\left\{(i\omega w)^* Q_x-\left[i\omega\left(\frac{\partial w}{\partial x}\right)\right]^* M_{xx}-\left[i\omega\left(\frac{\partial w}{\partial y}\right)\right]^* M_{xy}+(i\omega u)^* N_{xx}+(i\omega v)^* N_{xy}\right\}\mathrm{d}y. \tag{38}$$

From Eqs. (36a,b,c) and (37a,b,c), the flexural and in-plane displacements of the closed coupled plate structure is given by

$$w=w_{x0}F_0+w_{xs}F_s, \tag{39}$$

$$u=u_{x0}F_0+u_{xs}F_s, \tag{40}$$

$$v=v_{x0}F_0+v_{xs}F_s. \tag{41}$$

Substitution of Eqs. (39)–(41) into Eqs. (28)–(32), the following equations can be obtained:

$$M_{xx}=-D\left[\left(\frac{\partial^2 w_{x0}}{\partial x^2}+v\frac{\partial^2 w_{x0}}{\partial y^2}\right)F_0+\left(\frac{\partial^2 w_{xs}}{\partial x^2}+v\frac{\partial^2 w_{xs}}{\partial y^2}\right)F_s\right], \tag{42}$$

$$Q_x=-D\left[\left(\frac{\partial^3 w_{x0}}{\partial x^3}+\frac{\partial^3 w_{x0}}{\partial x\partial y^2}\right)F_0+\left(\frac{\partial^3 w_{xs}}{\partial x^3}+\frac{\partial^3 w_{xs}}{\partial x\partial y^2}\right)F_s\right], \tag{43}$$

$$M_{xy}=-D(1-v)\left(\frac{\partial^2 w_{x0}}{\partial x\partial y}F_0+\frac{\partial^2 w_{xs}}{\partial x\partial y}\right)F_s, \tag{44}$$

$$N_{xx}=-\frac{Eh}{(1-v^2)}\left[\left(\frac{\partial u_{x0}}{\partial x}+v\frac{\partial v_{x0}}{\partial y}\right)F_0+\left(\frac{\partial u_{xs}}{\partial x}+v\frac{\partial v_{xs}}{\partial y}\right)F_s\right], \tag{45}$$

$$N_{xy}=\frac{Eh}{2(1+v)}\left[\left(\frac{\partial u_{x0}}{\partial y}+\frac{\partial v_{x0}}{\partial x}\right)F_0+\left(\frac{\partial u_{xs}}{\partial y}+\frac{\partial v_{xs}}{\partial x}\right)F_s\right]. \tag{46}$$

Substitution of Eqs. (42)–(46) into Eq. (38), there is

$$\bar{I}_{xa} = -\frac{1}{2}\int_0^{L_y} \mathrm{Re}(AF_0^* F_0 + BF_0^* F_s + CF_s^* F_0 + HF_s^* F_s)\,\mathrm{d}y, \tag{47}$$

where

$$A = i\omega\left\{D\left[w_{x0}^*\left(\frac{\partial^3 w_{x0}}{\partial x^3}+\frac{\partial^3 w_{x0}}{\partial x\partial y^2}\right)-\frac{\partial w_{x0}^*}{\partial x}\left(\frac{\partial^2 w_{x0}}{\partial x^2}+\nu\frac{\partial^2 w_{x0}}{\partial y^2}\right)-(1-\nu)\frac{\partial w_{x0}^*}{\partial y}\frac{\partial^2 w_{x0}}{\partial x\partial y}\right]\right.$$
$$\left.-\frac{Eh}{(1-\nu^2)}u_{x0}^*\left(\frac{\partial u_{x0}}{\partial x}+\nu\frac{\partial v_{x0}}{\partial y}\right)-\frac{Eh}{2(1+\nu)}v_{x0}^*\left(\frac{\partial u_{x0}}{\partial y}+\frac{\partial v_{x0}}{\partial x}\right)\right\},$$

$$B = i\omega\left\{D\left[w_{x0}^*\left(\frac{\partial^3 w_{xs}}{\partial x^3}+\frac{\partial^3 w_{xs}}{\partial x\partial y^2}\right)-\frac{\partial w_{x0}^*}{\partial x}\left(\frac{\partial^2 w_{xs}}{\partial x^2}+\nu\frac{\partial^2 w_{xs}}{\partial y^2}\right)-(1-\nu)\frac{\partial w_{x0}^*}{\partial y}\frac{\partial^2 w_{xs}}{\partial x\partial y}\right]\right.$$
$$\left.-\frac{Eh}{(1-\nu^2)}u_{x0}^*\left(\frac{\partial u_{xs}}{\partial x}+\nu\frac{\partial v_{xs}}{\partial y}\right)-\frac{Eh}{2(1+\nu)}v_{x0}^*\left(\frac{\partial u_{xs}}{\partial y}+\frac{\partial v_{xs}}{\partial x}\right)\right\},$$

$$C = i\omega\left\{D\left[w_{xs}^*\left(\frac{\partial^3 w_{x0}}{\partial x^3}+\frac{\partial^3 w_{x0}}{\partial x\partial y^2}\right)-\frac{\partial w_{xs}^*}{\partial x}\left(\frac{\partial^2 w_{x0}}{\partial x^2}+\nu\frac{\partial^2 w_{x0}}{\partial y^2}\right)-(1-\nu)\frac{\partial w_{xs}^*}{\partial y}\frac{\partial^2 w_{x0}}{\partial x\partial y}\right]\right.$$
$$\left.-\frac{Eh}{(1-\nu^2)}u_{xs}^*\left(\frac{\partial u_{x0}}{\partial x}+\nu\frac{\partial v_{x0}}{\partial y}\right)-\frac{Eh}{2(1+\nu)}v_{xs}^*\left(\frac{\partial u_{x0}}{\partial y}+\frac{\partial v_{x0}}{\partial x}\right)\right\},$$

$$H = i\omega\left\{D\left[w_{xs}^*\left(\frac{\partial^3 w_{xs}}{\partial x^3}+\frac{\partial^3 w_{xs}}{\partial x\partial y^2}\right)-\frac{\partial w_{xs}^*}{\partial x}\left(\frac{\partial^2 w_{xs}}{\partial x^2}+\nu\frac{\partial^2 w_{xs}}{\partial y^2}\right)-(1-\nu)\frac{\partial w_{xs}^*}{\partial y}\frac{\partial^2 w_{xs}}{\partial x\partial y}\right]\right.$$
$$\left.-\frac{Eh}{(1-\nu^2)}u_{xs}^*\left(\frac{\partial u_{xs}}{\partial x}+\nu\frac{\partial v_{xs}}{\partial y}\right)-\frac{Eh}{2(1+\nu)}v_{xs}^*\left(\frac{\partial u_{xs}}{\partial y}+\frac{\partial v_{xs}}{\partial x}\right)\right\}.$$

By setting the partial derivatives of the active power flow with respect to the real and imaginary parts of the control force to be zero, the optimal control force can be obtained as follows:

$$F_s^{\mathrm{opt}} = -\frac{\int_0^{L_y} B^*\,\mathrm{d}y + \int_0^{L_y} C\,\mathrm{d}y}{2\int_0^{L_y}\mathrm{Re}(H)\,\mathrm{d}y}. \tag{48}$$

Substituting Eq. (48) into Eq. (47), the minimizing active power flow transmitted through the section x of the connected plate structure can be yielded. Of course, if the coordinate x is chosen at the junctions of the coupled plate, the time-average power transmitted through the junctions between the plates can be suppressed by Eqs. (47) and (48).

4. Numerical results and discussions

4.1. Active power at the junction of closed plate structure

The displacement responses and active power flow of the closed connected plate structure as shown in Fig. 1 are computed and suppressed with the active control method. The material parameters are $\nu=0.3$, $E=2.0\times10^{11}$ Pa and $\rho=7.8\times10^3$ kg/m^3. The structural damping factor is considered in the analysis by using the complex Young's modulus $E(1+i\eta)$, where $\eta=0.001$ is the structural damping factor. The width and thickness of the plate are $L_y=0.6$ m and $h=0.004$ m. The lengths of the plates are $L_1=L_2=L_3=L_4=1.6$ m. The disturbance $\vec{F}_0$ is located at $x_0=1$ m, $y_0=0.41$ m of plate 1, and the control force $\vec{F}_s$ is located at $x_s=1$ m, $y_s=0.2$ m of plate 1. In the calculation, $F_0=1$ N. The error sensor is located at $x_e=0.2$ m, $y_e=0.3$ m of plate 2.

To verify the validity of the proposed method, a comparison between the results obtained by FEM and the present method has been made. In the calculation of FEM, the rectangular element is used to disperse the connected rectangular plate structure. According to the finite element method, the discrete dynamical equation of the whole structure can be written as

$$[M]\{\ddot{q}\}+[C]\{\dot{q}\}+[K]\{q\}=\{f\} \tag{49}$$

where q is the nodal displacement matrix of the whole structure, $[M]$, $[C]$ and $[K]$ are the mass, damping and stiffness matrices of the whole structure and f is the force matrix. The modal analysis and vibration response of the structure can be calculated by finite element software (in this paper, the MSC. Nastran and Patran 2007 are used). The dynamical response in the mid-point of plate 3 of the connected plate structure with 1536 elements is calculated by the MSC. Nastran software and shown in Fig. 2.

Fig. 3 shows the response in the mid-point of plate 3 calculated by FEM and the proposed wave method. Different element numbers are used in FEM, such as 768 elements and 1536 elements. As shown in Fig. 3, with the increase of the

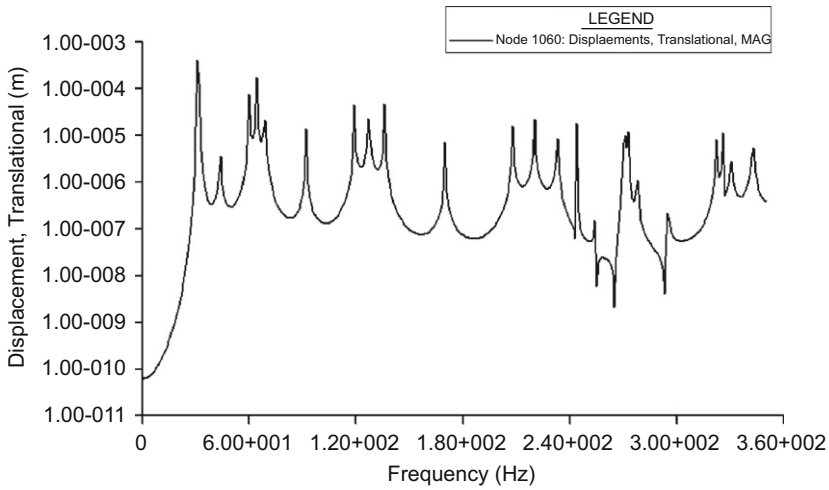

Fig. 2. The response of the mid-point in plate 3 calculated by 1536 elements with MSC. Nastran software.

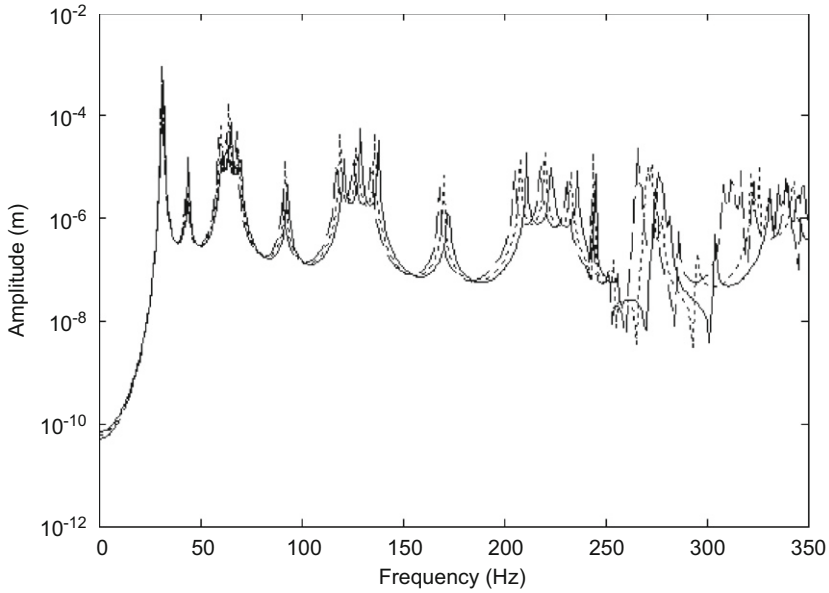

Fig. 3. Comparison of responses in □-shaped plate by FEM and wave method: (– – –) FEM: 768 elements; (------) FEM: 1536 elements; and (—) wave method.

element number in the FEM, the FEM results are convergent to the results of the wave method as the frequency increases. While all the results agree well with each other in the low frequency regions.

The FEM results agree with the results of the wave approach in low frequency regions in the coupled plate structure as shown in Fig. 2. And the FEM results are convergent to the results of wave method as the frequency increases. However, in the median and high frequency regions, the error of the results for FEM becomes larger as the frequency increases because of the uncertainty and the truncation error of the high-order modes. So, the results of FEM are not precise for the median and high frequencies even if more element numbers are employed. But the responses in the median and high frequency regions that satisfy the wave model assumption can be calculated by the wave approach.

In Fig. 4, the active control with different control forces is used to suppress the active power flow at the junction of the plates 1 and 2 in the closed connected plate structure in the lower frequency regions. As shown in Fig. 4, the results of the optimal control force are very good under 100 Hz, and above 100 Hz the control effects are very good near the resonate frequencies. The results of the optimal control force with 1 percent error are the same as those of the optimal control force above 100 Hz. It indicates that the active control effect of the active power transmitted through the junction of the closed connected plate is effective in lower frequency regions, and small error of control force has very slight influences on the control results.

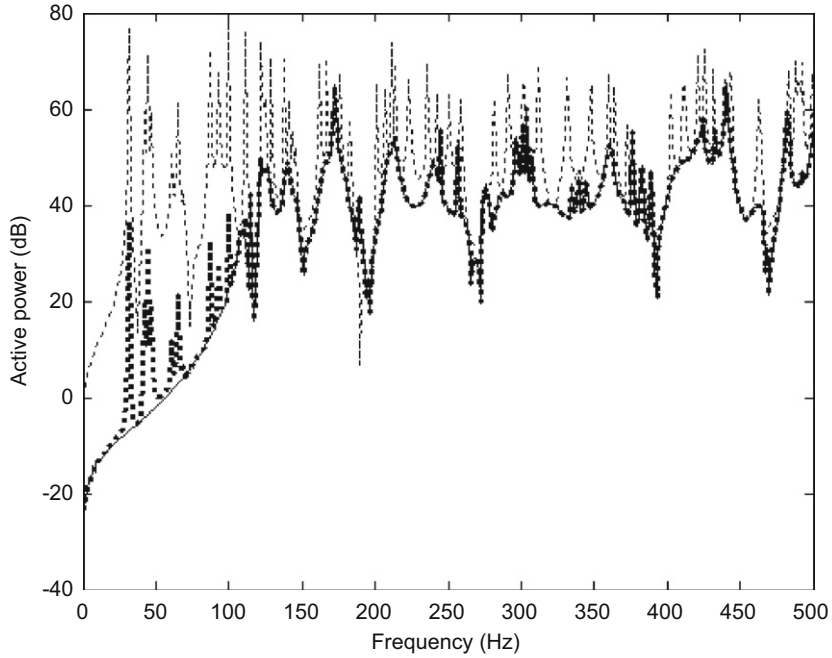

Fig. 4. Active control of the active power at junction of plates 1 and 2 in □-shaped plate with different control forces: without control force (----); 99 percent of optimal control force for minimizing the active power flow (■ ■ ■ ■); and optimal control force for minimizing the active power (—) (dB ref.: $10^{-10}w$).

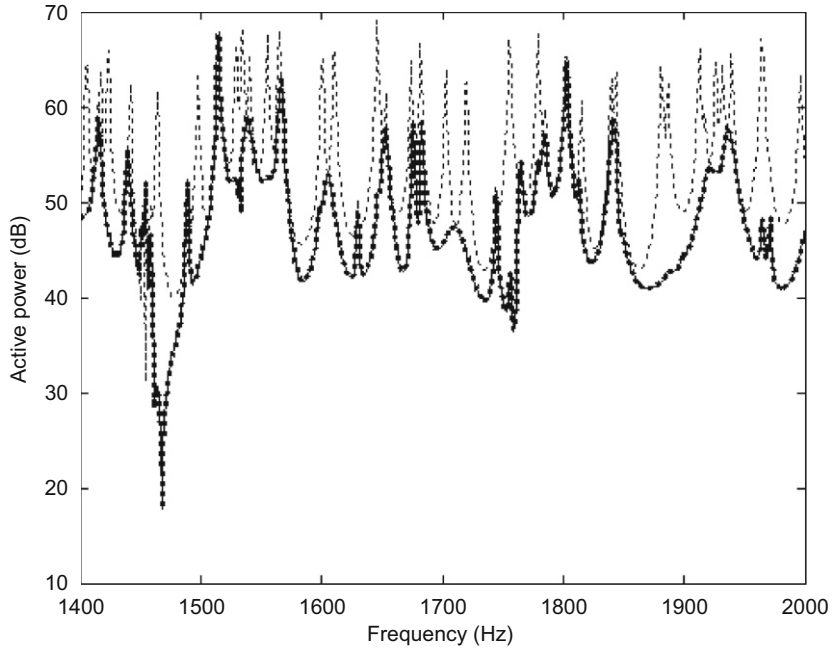

Fig. 5. Active control of active power at the junction of plates 1 and 2 in □-shaped plate with different control forces: without control force (----); 99 percent of optimal control force for minimizing the active power flow (■ ■ ■ ■); and optimal control force for minimizing the active power (—) (dB ref.: $10^{-10}w$).

In Fig. 5, the active control with different control forces is used to suppress the active power flow at the junction of plates 1 and 2 in the coupled plate structure for higher frequency regions. As shown in Fig. 5, the results of the optimal control force are very good near most of the resonate frequencies, and the results of the optimal control force with 1 percent error are the same as those of the optimal control force. It implies that the active control effect of the active power

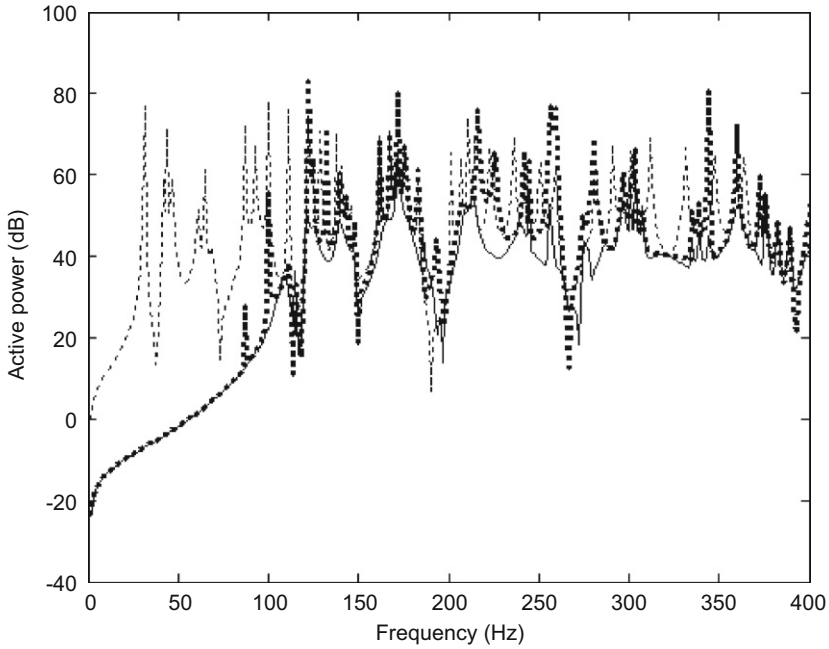

Fig. 6. Active control of active power at the junction of plates 1 and 2 in □-shaped plate with different control forces: without control force (----); optimal control force for minimizing the active power flow (■ ■ ■ ■); and optimal control force for minimizing the acceleration (—) (dB ref.: $10^{-10}w$).

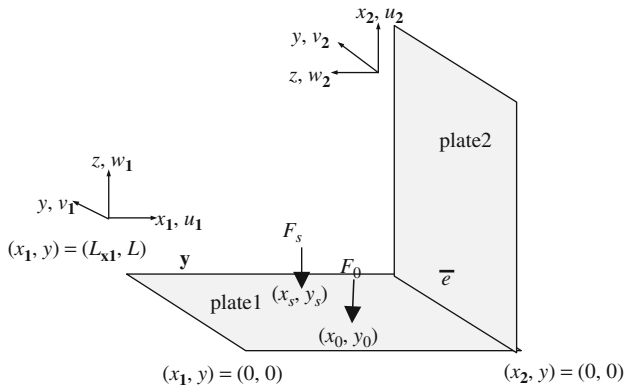

Fig. 7. The schematic diagram of L-shaped plate.

transmission through the junction of the closed connected plate structure is effective in higher frequency regions, and the control effect is not affected by small error of control force.

In Fig. 6, the active control with different control forces is used to suppress the active power transmitted through the junction of plates 1 and 2 in the closed connected plate structure. As shown in Fig. 6, for the optimal control force required to minimize the acceleration, the controlled active power flow is very good under 100 Hz. But above 100 Hz, the controlled active power flow is bigger than that without control force at many frequencies. While the control results of the optimal control force for minimizing the active power flow are better than those of the optimal control force for minimizing the acceleration in the whole frequencies. It indicates that the active power transmission through the junction of the closed connected plate structure can be well suppressed by the optimal control force for minimizing the active power flow.

4.2. Active power at the junction of L-shaped plate

The responses and active power flow of an L-shaped plate as shown in Fig. 7 are calculated and suppressed by the active control method. The material parameters are the same as those of the closed plate structure. The width and thickness of the plate are L_y=0.8 m and h=0.006 m. The length of the plates are L_1=1.6 m and L_2=1.2 m. The disturbance $\vec{F}_0$ is located at

x_0=0.8 m, y_0=0.3 m of the plate 1, and the control force $\vec{F}_s$ is located at x_s=0.8 m, y_s=0.5 m of plate 1. In the calculation, F_0=1 N. The error sensor is located at x_e=0.2 m, y_e=0.3 m of plate 2.

In Fig. 8, the responses of the mid-point in plate 2 are calculated by the FEM and wave method. Different element numbers are used in FEM, such as 224 elements and 768 elements. The results in Fig. 8 are similar to those in Fig. 3. With the increase of the element number in the FEM, the FEM results are convergent to the results of the wave method as the frequency increases. While all the results agree well with each other in the low frequency regions. It indicates that the structural vibration response in medium and high frequency regions can be more exactly computed by the wave method than by the FEM.

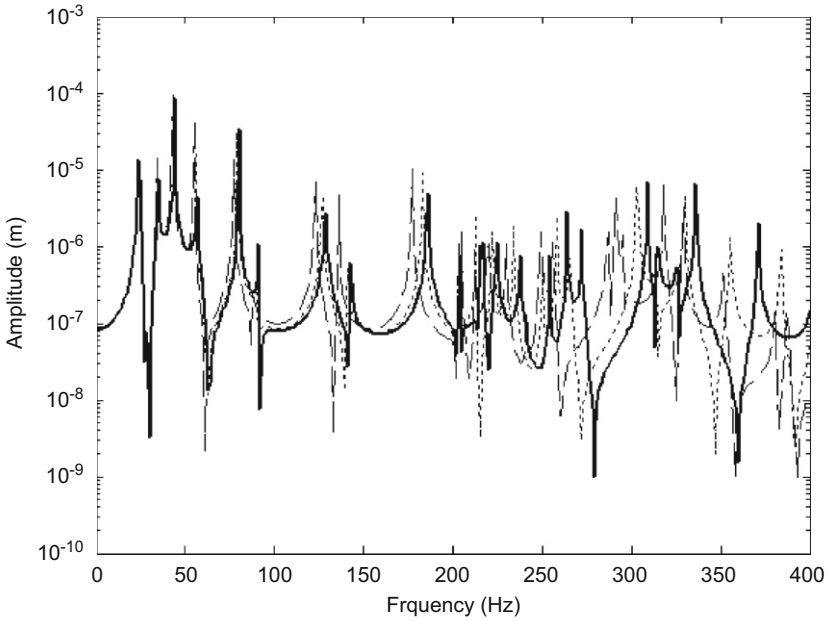

Fig. 8. Comparison of responses in L-shaped plate by FEM and wave method: (– – –) FEM: 224 elements; (------) FEM: 768 elements; and (—) wave method.

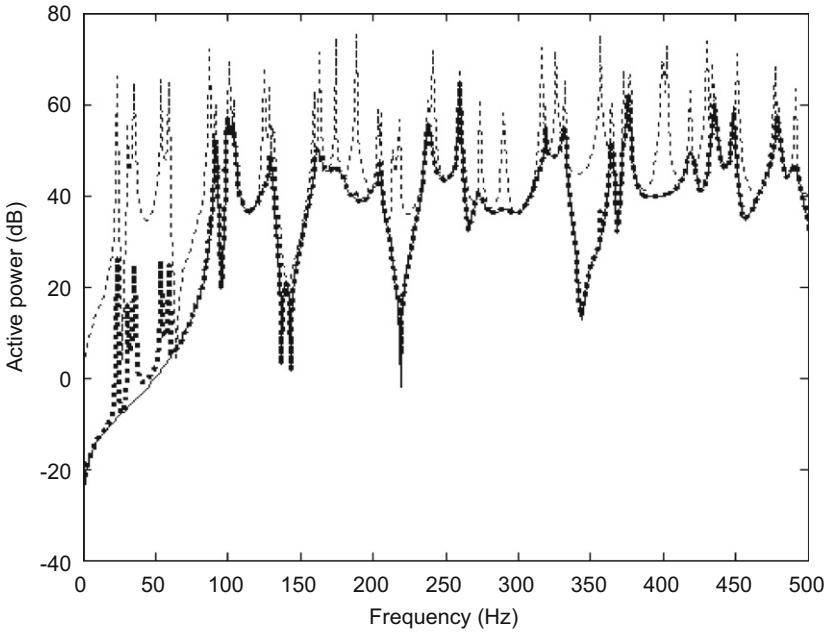

Fig. 9. Active control of the active power at junction of the L-shaped plate with different control forces: without control force (----); 99 percent of optimal control force for minimizing the active power flow (■ ■ ■ ■); and optimal control force for minimizing the active power (—) (dB ref.: $10^{-10}w$).

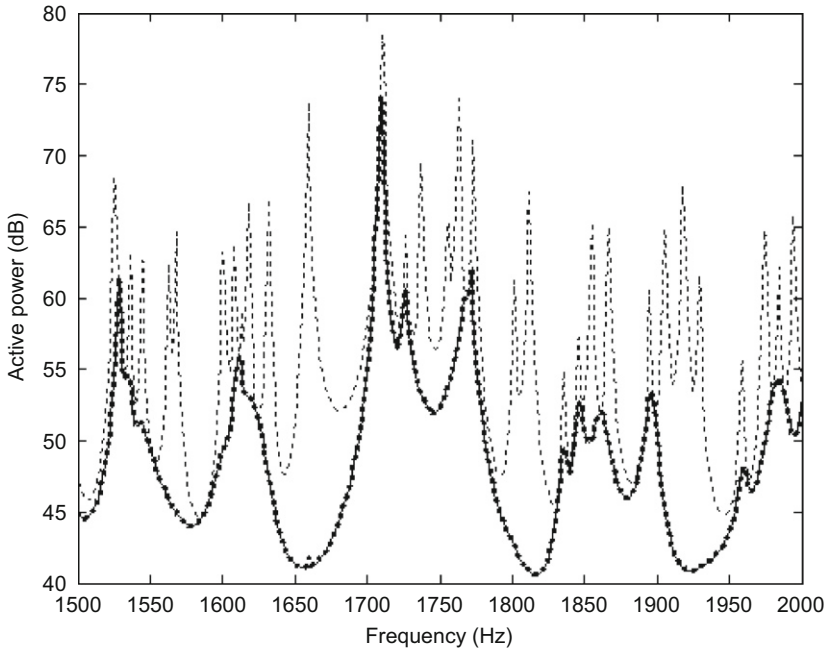

Fig. 10. Active control of the active power at junction of the L-shaped plate with different control forces: without control force (----); 99 percent of optimal control force for minimizing the active power flow (■ ■ ■ ■); and optimal control force for minimizing the active power (—) (dB ref.: $10^{-10}w$).

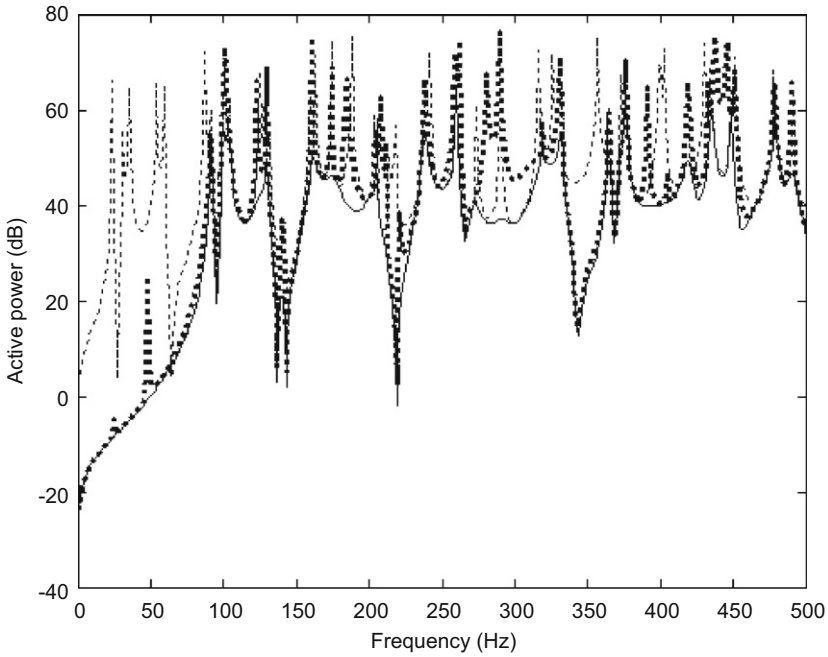

Fig. 11. Active control of the active power at junction of the L-shaped plate with different control forces: without control force (----); optimal control force for minimizing the active power flow (—); and optimal control force for minimizing the acceleration (■ ■ ■ ■) (dB ref.: $10^{-10}w$).

In Figs. 9 and 10, the active control with different control forces is used to suppress the active power flow at the junction of the L-shaped plate in the lower and higher frequency regions, respectively. As shown in Figs. 9 and 10, the results are similar to those in Figs. 4 and 5. It implies that the active power transmitted through the junction of the L-shaped plate can be effectively suppressed by the active control, and the control results are affected very slightly by the small error of control force.

In Fig. 11, the active control with different control forces is used to suppress the active power transmission through the junction of plates 1 and 2 in the L-shaped plate. As shown in Fig. 11, the results are similar to those in Fig. 6. It shows that the control effect by the optimal control force for minimizing the active power flow is better than that by the optimal control force for minimizing the acceleration.

5. Conclusions

The dynamic responses of the connected plate structures are investigated by the wave method. The disturbance propagation at the junction of the connected plates is suppressed by active control for minimizing active power flow. The conclusions can be drawn as follows:

(1) The response of the finite connected plate structure in the medium and high frequencies can be calculated by the wave method.
(2) The active power flow through the junction of the connected plate structure can be effectively suppressed by the control force for minimizing the active power flow. And the control effect by the optimal control force for minimizing the active power flow is better than that by the optimal control force for minimizing the acceleration.
(3) Small error of the optimal control force for minimizing the active power flow has slight influences in low frequencies, but no effects in medium and high frequency regions on the active control of the energy propagation through the junction of the finite coupled plate structure.

Acknowledgements

The authors wish to express gratitude for the supports provided by the National Natural Science Foundation of China under Grant nos. 10672017 and 10632020 for this research work.

References

[1] D.U. Noiseux, Measurement of power flow in uniform beams and plates, *The Journal of the Acoustical Society of America* 47 (1) (1970) 238–247.
[2] Y.H. Park, S.Y. Hong, Vibrational power flow models for transversely vibrating finite Mindlin plate, *Journal of Sound and Vibration* 317 (2008) 800–840.
[3] A.J. Romanoa, P.B. Abraham, E.G. Williams, A Poynting vector formulation for thin shells and plates, and its application to structural intensity analysis and source localization—part I: theory, *The Journal of the Acoustical Society of America* 87 (3) (1990) 1166–1175.
[4] B.R. Mace, Power flow between two continuous one-dimension subsystems: a wave solution, *Journal of Sound and Vibration* 154 (2) (1992) 289–319.
[5] B.R. Mace, The statistics of power flow between two continuous one dimension subsystems, *Journal of Sound and Vibration* 154 (2) (1992) 321–341.
[6] M.D. McCollum, J.M. Cuschieri, Bending and in-plane wave transmission in thick connected plates using statistical energy analysis, *The Journal of the Acoustical Society of America* 88 (3) (1990) 1480–1485.
[7] J.M. Cuschieri, Structural power-flow analysis using a mobility approach of an L-shaped plate, *The Journal of the Acoustical Society of America* 87 (3) (1990) 1159–1165.
[8] J.M. Cuschieri, M.D. McCollum, Thick plate bending wave transmission using a mobility power flow approach, *The Journal of the Acoustical Society of America* 88 (3) (1990) 1472–1479.
[9] J.M. Cuschieri, Parametric analysis of the power flow on an L-shaped plate using a mobility power flow approach, *The Journal of the Acoustical Society of America* 91 (5) (1992) 2686–2695.
[10] J.M. Cuschieri, M.D. McCollum, In-plane and out-of-plane waves' power transmission through a L-plate junction using the mobility power flow approach, *The Journal of the Acoustical Society of America* 100 (2) (1996) 857–870.
[11] N.J. Kessissoglou, Power transmission in L-shaped plates including flexural and in-plane vibration, *The Journal of the Acoustical Society of America* 115 (3) (2004) 1157–1169.
[12] W.J. Choi, Y.P. Xiong, R.A. Shenoi, Power flow analysis for a floating sandwich raft isolation system using a higher-order theory, *Journal of Sound and Vibration* 319 (2009) 228–246.
[13] J. Yan, T.Y. Li, J.X. Liu, X. Zhu, Input power flow in a submerged infinite cylindrical shell with doubly periodic supports, *Applied Acoustics* 69 (2008) 681–690.
[14] J. Yan, F.Ch Li, T.Y. Li, Vibrational power flow analysis of a submerged viscoelastic cylindrical shell with wave propagation approach, *Journal of Sound and Vibration* 303 (2007) 264–276.
[15] J. Pan, C.H. Hansen, Active control of total vibratory power flow in a beam—I: physical system analysis, *The Journal of the Acoustical Society of America* 89 (1) (1991) 200–209.
[16] X. Pan, C.H. Hansen, The effect of error sensor location and type on the active control of beam vibration, *Journal of Sound and Vibration* 165 (3) (1993) 497–510.
[17] A.E. Schwenk, S.D. Sommerfeldt, S.I. Haye, Adaptive control of structural intensity associated with bending waves in a beam, *The Journal of the Acoustical Society of America* 96 (5) (1994) 2826–2835.
[18] P. Audrain, P. Masson, A. Berry, Investigation of active structural intensity control in finite beams: theory and experiment, *The Journal of the Acoustical Society of America* 108 (2) (2000) 612–623.
[19] A.K.A. Pereira, F.J.O. Moreiraf, J.R.F. Arruda, Active control of the structural intensity in beams using a frequency domain adaptive method, *AIAA* 1798 (1998) 841–849.
[20] X. Pan, C.H. Hansen, Active control of vibratory power transmission along a semi-infinite plate, *Journal of Sound and Vibration* 184 (4) (1995) 585–610.
[21] A.N. Bercin, R.S. Langley, Application of the dynamic stiffness technique to the in-plane vibrations of plate structures, *Computers and Structures* 59 (5) (1996) 869–875.
[22] J. Keir, N.J. Kessissoglou, C.J. Norwood, Active control of connected plates using single and multiple actuators and error sensors, *Journal of Sound and Vibration* 281 (2005) 73–97.
[23] C.Q. Howard, S.D. Snyder, C.H. Hansen, Calculation of vibratory power transmission for use in active vibration control, *Journal of Sound and Vibration* 233 (4) (2000) 573–585.